Human Somatostatin Receptor Specificity of Backbone-Cyclic Analogues Containing Novel Sulfur Building Units

Sharon Gazal,[†] Garry Gelerman,[‡] Ofer Ziv,[‡] Olga Karpov,[‡] Pninit Litman,[‡] Moshe Bracha,[‡] Michel Afargan,*[,‡] and Chaim Gilon*[,†]

Department of Organic Chemistry, Hebrew University, Jerusalem 91904, Israel and Peptor Ltd., Kiryat Weizmann, Rehovot 76326 Israel

Received January 22, 2001

Somatostatin-14 (somatostatin) and its clinically available analogues octreotide, lanreotide, and vapreotide are potent inhibitors of growth hormone, insulin, and glucagon release. Recently, a novel backbone cyclic somatostatin analogue c(GABA-Phe-Trp-(D)Trp-Lys-Thr-Phe-GlyC3-NH_2) (analogue **1**, PTR 3173) that possesses in vivo endocrine selectivity was described. This long-acting octapeptide exhibits high affinity to human recombinant somatostatin receptors (hsst) hsst2, hsst4, and hsst5. Its novel binding profile resulted in potent in vivo inhibition of growth hormone but not of insulin release. We report the synthesis, bioactivity, and structure−activity relationship studies of compounds related to **1**. In these analogues, the lactam bridge of **1** was replaced by a backbone disulfide bridge. We present a novel approach for conformational constraint of peptides by utilizing sulfur-containing building units for on-resin backbone cyclization. These disulfide backbone cyclic analogues of **1** showed significant metabolic stability as tested in various enzyme mixtures. Receptor binding assays revealed different receptor selectivity profiles for these analogues in comparison to their prototype. It was found that analogues of **1**, bearing a disulfide bridge, had increased selectivity to hsst2 and hsst5; however, they exhibited weaker affinity to hsst4 as compared to **1**. These studies imply that ring chemistry, ring size, and ring position of the peptide template may affect the receptor binding selectivity.

Introduction

In many naturally occurring cyclic peptides, conformational constraints are obtained by a disulfide bridge.[1−3] Replacement of the disulfide bridge by an amide bond may retain conformational constraint.[4] However, it may also alter physicochemical properties of the peptide due to the addition of potential hydrogen-bonding sites through the bridge and consequent increase of ring polarity.[4,5] It was suggested that the physicochemical alterations might create undesirable effects on pharmacological activities of the peptide.[6−8] These arguments also apply to backbone cyclic peptides in drug development[4,5,8,9] hence the extensive search for backbone cyclic drug candidates and the attendant issues of pharmacological properties of these peptidomimetics.[9−12]

Somatostatin is a tetradecapeptide, which inhibits the release of various hormones and enzymes.[13−15] Synthetic somatostatin analogues, which were developed for clinical use, share with the native peptide its pharmacophore, the essential amino acid sequence Phe^7-Trp^8-Lys^9-Thr^{10} responsible for efficacy (the numbering refers to the location of the residues in native somatostatin[16]). To date, the three somatostatin drugs octreotide ((SMS201995)−[DPhe-Cys-Phe-DTrp-Lys-Thr-Cys-Thr-(ol)]), lanreotide ((BIM 23014)−[DNal-Cys-Tyr -DTrp-Lys-Val-Cys-Thr-NH_2]), and vapreotide ((RC160)−[DPhe-Cys-Tyr-DTrp-Lys-Val-Cys-Trp-NH_2]) have been shown to be effective in various endocrine and gastrointestinal abnormalities.[17] These somatostatin analogues all have similar binding affinities for four of the five human somatostatin receptor subtypes (hsst): high affinity for hsst2 and hsst5, moderate affinity for hsst3, and very low affinity for hsst1. Lanreotide and vapreotide have a moderate affinity for hsst4, whereas octreotide has little or no affinity for this human somatostatin receptor.[14,17] This family of drugs inhibits the endocrine release of growth hormone, glucagon, and insulin with high potency in comparison to the native somatostatin.[14,15,17]

Recently, a novel, backbone cyclic, long-acting somatostatin analogue, **1**, with improved pharmacological properties was described.[18] Analogue **1** is 1000- and 10 000-fold more potent in the in vivo inhibition of growth hormone than of glucagon and of insulin release, respectively. In fact, **1** is the first somatostatin analogue that possesses complete in vivo selectivity between growth hormone and insulin inhibition. The binding profile of **1**, namely, the combination of receptor subtypes to which the analogue binds with high affinity, is different than other somatostatin analogues such as octreotide, lanreotide, and vapreotide.

In this study, we have reintroduced the original disulfide bridge that exists in somatostatin and in most of its potent synthetic analogues. We describe the synthesis and bioactivity of metabolically stable, receptor selective, backbone cyclic, disulfide bridged somatostatin analogues based on the sequence of **1**. These

* To whom correspondence should be addressed. (C.G.) Tel.: 972-2-6586181. Fax: 972-2-6585345. E-mail: gilon@vms.huji.ac.il. (M.A.) Tel.: 972-8-9409451. Fax: 972-8-9409452. E-mail: hpbm@netvison.net.il.
[†] Hebrew University.
[‡] Peptor Ltd.

10.1021/jm0100281 CCC: $22.00
Published on Web 03/16/2002

Analogue number	Subgroup	Mode of Cyclization*	Ring size**	Structure
(1)	i	AE-BN	8+20 (28)	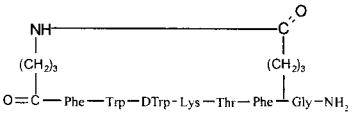
(2) n=1 (3) n=2	i	AE-BN	5+20 (25) 6+20 (26)	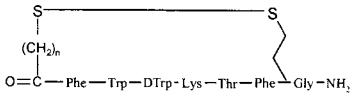
(4) Xaa= 0 (5) Xaa= D-Phe	ii	SC-BN	5+21 (26)	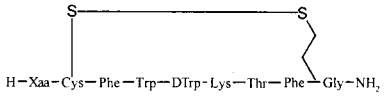
(6) Xaa= 0 (7) Xaa= D-Phe (8) Xaa= D-Nal	iii	BN-BN	6+22 (28)	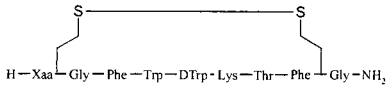

Figure 1. Structure of the various backbone cyclic somatostatin analogues. The single asterisk denotes the AE-BN amino end to backbone nitrogen, SC-BN side chain to backbone nitrogen, and BN-BN backbone nitrogen to backbone nitrogen. The double asterisk denotes the number of atoms in the bridge + number of atoms in the backbone (total number of atoms in the ring).

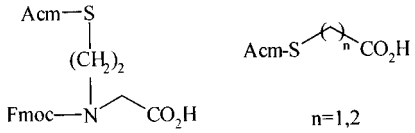

Figure 2. Structures of the Fmoc-N$^{\alpha}$-[ω(Acm)-S-alkyl]Gly-OH building unit and Acm-protected thioalkyl carboxylic acids.

analogues were prepared by incorporation of a novel sulfur-containing acetamidomethyl (Acm)-protected building unit.

Results

Design of the Backbone Cyclic Analogues of 1. Our synthetic approach for novel backbone cyclic disulfide bridged somatostatin analogues was made possible due to the development of novel sulfur-containing building units (Figure 2). The GlyC3 (Figure 1) and GABA terminals of **1** were substituted with GlyS2, Cys, thioacetic, and thioapropanoic acids.

Building Blocks Synthesis. The synthesis of the thiol-containing building blocks for the preparation of the disulfide bridged backbone cyclic analogues is described in Figure 3. The synthesis of Fmoc-GlyS2-(Acm)-OH {9-flourenylmethoxycarbonyl-GlyS2(Acm)-OH}, which was incorporated into all of the disulfide bridged analogues, came out as follows: reaction of the commercially available thioethylamine (**1**) with acetamidomethanol in trifluoroacetic acid (TFA) yielded the Acm-protected thioethylamine (**2**), followed by reductive alkylation of the primary amine with glyoxylic acid in the presence of sodium cyanoborohydride. Finally, the α amine was protected by reaction of **3** with Fmoc-OSu in a MeCN/H_2O mixture in the presence of Et_3N.

Acm−thioacetic acid was prepared in order to obtain the backbone-to-end disulfide bridged analogue 2 (Figure 1). This compound was obtained by reaction of the commercially available thioacetic acid (**5**) with acetamidomethanol in TFA as described in Figure 3b. Similarily, Acm−thiopropanoic acid (**9**) was prepared in order to obtain the backbone-to-end disulfide bridged analogue 3 (Figure 1). This compound was obtained by

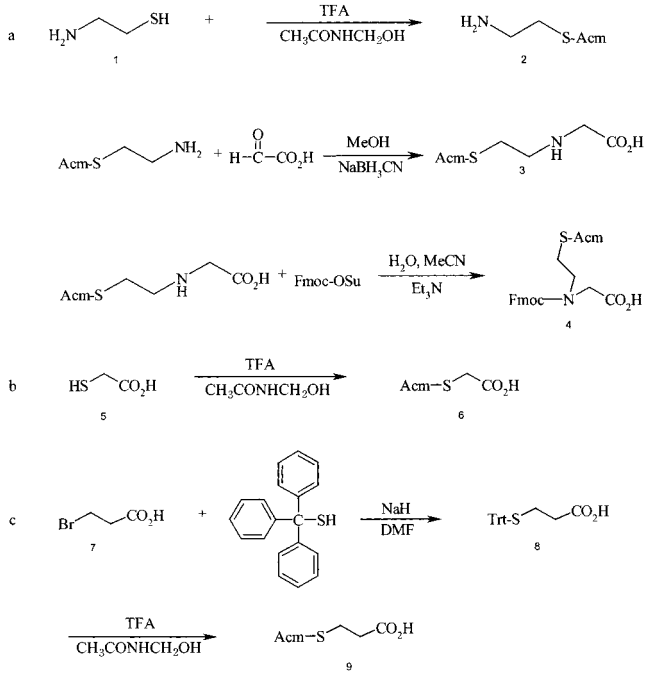

Figure 3. Synthesis of the building blocks for the disulfide bridged backbone cyclic analogues.

the reaction of the commercially available bromopropanoic acid and trityl mercaptan in the presence of sodium hydride in dimethylformamide (DMF) yielding the triphenylmethyl (Trt)-protected thiopropanoic acid (**8**) (Figure 3c). In situ replacement of Trt by Acm was then accomplished by reaction of **8** with acetamidomethanol in TFA as described in Figure 3c.

Peptide Synthesis. Peptide assembly was carried out using the standard solid phase methodology with Fmoc chemistry. N-alkylated Gly residues containing an Acm-protected thioethyl group on the α amino group Fmoc-GlyS2(Acm)-OH were incorporated in the carboxy terminal position. An additional Acm-protected thiol group was incorporated in the amino terminus (position 1 or 2). Following peptide elongation, the formation of a disulfide bridge and removal of Acm groups were

Table 1. IC_{50} Values (nM) of the Displacement of [^{125}I] Tyr^{11} Somatostatin-14 Binding by **1** and the Various Backbone Cyclic Somatostatin Analogues Containing Disulfide Bridges

receptor/ analogue no.	hsst1	hsst2	hsst3	hsst4	hsst5
1	>1000	3 ± 0.75	>100	7 ± 1.1	1 ± 0.05
2	>1000	28.7 ± 2.17	15.6 ± 2.1	>100	1.3 ± 0.08
3	>1000	1.3 ± 0.05	>100	>100	2.8 ± 0.4
4	>1000	5.2 ± 0.6	40.7 ± 2.17	41.1 ± 3.2	1.2 ± 0.1
5	>1000	12.8 ± 1.9	>100	35.9 ± 2.8	4.5 ± 0.7
6	>1000	4.1 ± 0.6	>100	49.5 ± 3.4	7.8 ± 1.3
7	>1000	2.5 ± 0.3	>100	>100	18.2 ± 1.8
8	>1000	8.4 ± 1.5	>100	61.8 ± 2.9	91 ± 3.3

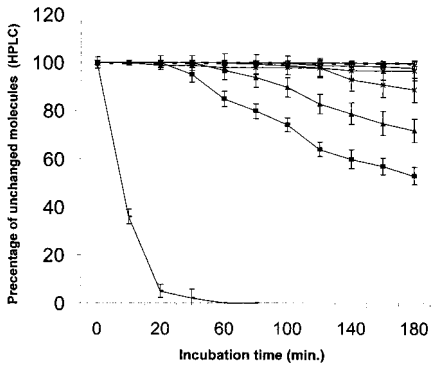

Figure 4. Biostability of somatostatin and its backbone cyclic analogues in renal homogenate. 1 (- - -), 2 (○), 3 (▲), 4 (*ν*), 5 (×), 6 (*ς*), 7 (□), and somatostatin (—).

carried out in situ with the peptide attached to the solid support.[19,20]

Biological Activity. The affinities of the backbone cyclic peptides to the five humane somatostatin receptors were determined using receptor binding assays in which the tested analogue competes for the binding of radiolabeled somatostatin to human cloned receptors expressed in CHO-K1 cells. Table 1 depicts the IC_{50} values calculated for the various backbone cyclic peptides for each of the five somatostatin receptors.

Metabolic Stability. The metabolic stability of the backbone cyclic analogues was studied in biological media known to have broad enzymatic degradation activity (rat liver and renal homogenate), as compared to enzymatic free buffer (Tris-HCl, pH 7.4). Six of the seven analogues were tested. These analogues showed significant resistance to enzymatic degradation after 3 h in renal and liver homogenate (see Figure 4) as compared to the fast decay of somatostatin under the same experimental conditions. The least stable peptide was analogue 4 that showed $t_{1/2}$ of 3 h in renal homogenate, while somatostatin was degraded within 10 min under these conditions.

Discussion

Recently, a novel backbone cyclic, high affinity ligand of the human somatostatin receptors was described.[18] This ligand, **1** (see Figure 1), is equipotent to other long-acting somatostatin analogues in the inhibition of growth hormone release. However, in contrast to the clinically available somatostatin analogues that are also potent inhibitors of insulin and glucagon release, **1** is 10 000-fold more potent in the in vivo inhibition of growth hormone over insulin and 1000-fold more potent in the in vivo inhibition of growth hormone vs glucagon release. Analogue **1** is the first long-acting somatostatin analogue showing complete in vivo selectivity between growth hormone and insulin inhibition. So far, the correlation between binding to a single somatostatin receptor and particular physiological activity could not be elucidated. Therefore, a novel approach termed "profile selectivity" was suggested by Afargan et al.[18] It was suggested that profile selectivity, namely, in vitro selectivity to receptor subset, rather than single receptor subtype, could dissociate the physiological effects mediated by somatostatin analogues. Many somatostatin analogues have profile selectivity to receptors hsst2, hsst3, and hsst5, and even single receptor selective analogues have been reported.[21] However, in vivo studies revealed that none of these analogues shows physiological selectivity,[22,23] while the unique profile selectivity to hsst2, hsst4, and hsst5 exhibited by **1** led to physiological selectivity. It was suggested that the unique pharmacology of **1** may provide a new pharmacotherapy approach for various endocrine abnormalities where the endocrine nonselective somatostatin analogues are not efficient.

In this paper, we have used **1** as a basis for structure—activity relationship studies in order to discover leads with new types of profile selectivity. Here, we describe the synthesis and biological activity of analogues of **1** containing a disulfide bond ring replacing the original lactam bridge. For this purpose, we have synthesized a novel class of thiol-containing protected building units for backbone cyclization as well as Acm-protected thioalkyl carboxylic acids (see Figure 3). The building units were incorporated into the analogues by standard solid phase peptide synthesis methods using Fmoc chemistry and bromo-tris-pyrrolidone-phosphonium hexafluorophosphate (PyBroP) as a coupling agent. Coupling of the building unit proceeded smoothly when the building unit was either coupled directly to the resin or coupled to peptidyl resin. Coupling to the building unit resin or building unit peptidyl resin also proceeded without any difficulties using standard PyBroP-mediated coupling. Analogue 4 was used as a model to fine tune the conditions of the "on-resin" Acm deprotection/oxidation reaction. Two methods were compared using iodine and $Tl(CF_3COO^-)_3$ as deprotection/oxidation agents.[20,24] Both reagents furnished the desired monocyclic analogues in high yield and homogeneity. HPLC (high-performance liquid chromatography)/MS (mass spectrometry) analysis of the analogues did not reveal extensive formation of dimers or oligomers. It seems that the introduction of the novel N-(*ω*-thioalkylated) amino acid in the ring increased the propensity of these analogues to undergo monocyclization rather than dimerization or oligomerization. The other six analogues were oxidized using the

less toxic iodine since it gave the same results as $Tl(CF_3COO^-)_3$. Protecting the indol functional group of Trp residues with Boc efficiently prevented its oxidation during the formation of the disulfide bond.

Structure−Activity Relationship Studies. Analogue **1** and its disulfide bridged analogues presented in this work share the common core sequence Phe-Trp-DTrp-Lys-Thr-Phe-Gly-NH_2 as well as the position of the bridge branching from the backbone nitrogen of the C terminal Gly residue. Several features such as ring chemistry, ring size, ring location, and the amino terminus character were investigated in order to elucidate the chemical properties that lead to the unique profile selectivity of **1**.

The analogues were divided into three subgroups according to their mode of cyclization (Figure 1). Subgroup (i) consisted of the amino end to backbone nitrogen cyclization mode, subgroup (ii) featured side chain to backbone nitrogen cyclization while subgroup (iii) included peptides with the backbone nitrogen to backbone nitrogen cyclization mode.

In each subgroup, the cyclization position is shifted toward the N terminus by one atom at a time. In subgroup (i) (analogues 2 and 3), the cyclization position is located on the carbonyl moiety preceding the N terminal Phe, in a similar location as in **1**. In subgroup (ii) (analogues 4 and 5), the cyclization position is located on the C^α of the amino acid preceding the N terminal Phe. In subgroup (iii) (analogues 6−8), the cyclization position is located on the N^α of the Gly preceding the N terminal Phe. In addition to the effect of the cyclization position and ring size on profile selectivity, other parameters such as additional positive charge and/or additional amino acid were assessed.

Analogues 2 and 3 comprise similar sequence and cyclization positions as in **1**. However, these analogues differ from **1** in two parameters: (i) the number of atoms in the ring. Analogues 2 and 3 feature rings shorter by 3 and 2 carbon bonds, respectively. Decreasing ring size was performed in order to compensate for the increase in bond length and van der Waals radii induced by the disulfide bond as compared to the amide bond. Thus, in these analogues, an attempt was made to maintain similar ring size to that of the parent peptide **1**.

(ii) The spatial position of the amide bond in **1** relative to the backbone is different from that of the disulfide bond in analogues 2 and 3. This difference is induced by the difference in ring sizes of these compounds.

The profile selectivity of **1** indicates high affinity binding to receptors hsst2, hsst4, and hsst5. While the affinity to receptors hsst2 and hsst5 is maintained, all of the disulfide bridged analogues show lower affinity to hsst4; hence, they possess different profile selectivity. In addition, analogues 2 and 4 show high to moderate affinity to hsst3, which is not observed with the parent compound **1**.

Analogue 2 shows IC_{50} values of 28.7 and 15.6 nM to receptors hsst2 and hsst3, respectively. The selectivity between these two receptors is dramatically improved in analogue 3 (which has a larger ring size). This analogue is selective between receptors hsst2 and hsst3 as the parent analogue.

Analogue 4 has the same ring size as analogue 3, with a different cyclization position and an additional positively charged amino group. These modifications led to a change in profile selectivity whereas analogue 4 binds receptor hsst3 (40.7 nM) and receptor hsst4 (41.1 nM). Similarly, **1** and analogue 6 have the same ring size, but analogue 6 has a different cyclization position and a positively charged secondary amine. As mentioned above, these analogues also differ in their ring chemistry. Both analogues display a similar profile selectivity except that the IC_{50} of analogue 6 for hsst4 is decreased, 49.5 nM, as compared to 7 nM of **1**.

Analogues 5, 7, and 8 have hydrophobic D amino acid on their N terminus. The addition of DPhe to analogue 4 resulted in lower affinity toward hsst3 but had a small effect on the affinity to hsst2 and hsst5 receptors. On the other hand, the addition of DPhe or DNal to analogue 6, to yield analogues 7 and 8, respectively, had a remarkable effect on the affinity to hsst5. Analogue 8 is thus selective to the hsst2 receptor and moderately selective to receptors hsst4 and hsst5.

Introducing hydrophobic moieties preceding the second building unit also affected the profile selectivity by lowering the affinity to hsst5. Furthermore, the most hydrophobic analogue 8 had the lowest affinity to hsst5 leading to a change in profile selectivity.

Stability toward Enzymatic Degradation. All of the analogues (except analogue 8 that was not determined) were found to be metabolically stable in renal and liver homogenates while native somatostatin degraded almost completely within 10 min under these conditions. The improved stability toward severe proteolytic activity is in agreement with our expectations of backbone cyclic peptides.

Conclusions

We have prepared a series of cyclic somatostatin analogues based on the sequence of the novel endocrine selective somatostatin analogue, **1**. We have shown that the replacement of lactam with a disulfide bridge retains metabolic stability in most of the peptides (Figure 4). However, it significantly affects the receptor binding specificity motif of **1**. For the synthesis of these analogues, we have prepared novel sulfur Acm-protected building units. These building units enable us to increase the diversity of backbone cyclic libraries and provide the ability to create bicyclic peptides that contain both amide and disulfide bridges leading to more rigid structures.

Experimental Section

Abbreviations. N^α-(ω-functionalized alkyl-) amino acid building units within a peptide chain are abbreviated by a three letter abbreviation of the amino acid residue, followed by one letter that designates the function on the ω alkyl chain and a number that designates the length of the alkyl chain. For example, N^α-(ω-S-ethyl)Gly refers to GlyS2. Protected building units are abbreviated as follows: a protecting group on N^α is introduced prior to the abbreviation of the amino acid. A protecting group on the ω alkyl functional group is introduced in brackets after the number of the alkyl groups. For example: Fmoc-N^α-[ω(Acm)-S-ethyl]Gly-OH is abbreviated as Fmoc-GlyS2(Acm)-OH.

Building Blocks Synthesis. Acm−Thioethylamine (2). Cysteamine hydrochloride (compound **1**, Figure 3) (20 g, 0.176 mol) was dissolved in 140 mL of TFA. The solution was stirred at room temperature for 30 min. Then, a solution of acetamidomethanol (16.38 g, 0.184 mol) in 40 mL of TFA was added. The mixture was stirred for an additional 2.5 h. Most of the

TFA was evaporated, and 800 mL of triple-distilled water (TDW) was added. The solution was cooled by ice bath and brought to pH 9 by concentrated ammonium hydroxide and then saturated with NaCl. The product was extracted with six portions of 400 mL of chloroform:2-propanol 3:1. The organic phase was dried over Na_2SO_4, evaporated to dryness, and put in a desiccator overnight, yielding 12.25 g (0.083 mol 47%) of yellow oil. ^{1}H nuclear magnetic resonance (NMR) (CD_3OD, 300 MHz 298 K): δ 1.95 (s, 3H), 2.69 (t, 2H), 2.86 (t, 2H), 4.30 (s, 2H).

Fmoc-N$^{\alpha}$-[ω(Acm)-S-ethyl]glycine-OH (4). Compound **2** (0.1 mol) and $NaBH_3CN$ (6.3 g, 0.1 mol) were dissolved in 200 mL of MeOH, followed by the addition of glyoxilic acid monohydrate (7.8 g, 0.085 mol). The solution was stirred for 19 h, and the MeOH was evaporated. The oil obtained was dissolved in 250 mL of TDW, and Et_3N (24 mL, 0.17 mol) was added. To this mixture, a solution of 21.5 g (0.064 mol) of Fmoc-Osu, dissolved in 375 mL of MeCN, was added, and the solution was stirred for 4 h. A small portion of the MeCN was evaporated, and the pH was found to be 9. The solution was washed with 3 × 400 mL of petroleum ether (40−60) followed by 3 × 400 mL of ether:petroleum ether (40−60) 7:3; the solution was brought under cooling to pH 3−4 using HCl 2 N and extracted by 4 × 350 mL of ethyl acetate. The ethyl acetate phase was washed by 3 × 250 mL of HCl 1 N and 3 × 250 mL of saturated $KHSO_4$ solution, dried over Na_2SO_4, and evaporated resulting in a white solid (10 g 37%); mp 139−145 °C. ^{1}H NMR (CD_3OD, 300 MHz 298 K, isomer ratio E:Z = 1:1): δ 1.90 (s, 1.5H), 1.95 (s, 1.5H), 2.32 (t, 1H), 2.73 (t, 1H), 3.22 (t, 1H), 3.51 (t, 1H), 3.95 (s,1H), 4.00 (s, 1H), 4.15 (s, 1H), 4.20 (t, 0.5H), 4.26 (t, 0.5H), 4.30 (s, 1H), 4.37 (d, 1H), 4.55 (d, 1H) 7.29−7.81 (m, 8H). MS (FAB): m/z 428.

Acm−Thioacetic Acid (6). Thioacetic acid (**5**) (12.51 mL, 0.18 mol) was dissolved in 100 mL of TFA. The solution was stirred for 30 min at room temperature. A solution of acetamidomthanol (16.5 g, 0.185 mol) in 40 mL of TFA was then added. The solution was stirred overnight. Most of the TFA was evaporated, and 300 mL of water was added. The solution was saturated with NaCl and brought to pH 3 using Na_2CO_3. The product was extracted to four portions of 300 mL of chloroform:2-propanol (3:1), and the organic phase was dried over Na_2SO_4 and evaporated yielding 14.97 g (0.092 mol 51.1%) of white oil. ^{1}H NMR (CD_3OD, 300 MHz): δ 1.95 (s, 3H), 3.36 (s, 2H), 4.39 (s, 2H).

Trityl−Thiopropanoic Acid (8). Trityl mercaptan (36.13 g, 0.131 mol) was added stepwise to a suspension of NaH (11.5 g, 60% in mineral oil 0.288 mol) in 80 mL of DMF under cooling and a nitrogen atmosphere, and the reaction mixture was stirred for 30 min after the addition was completed. A solution of bromopropionic acid (**7**) (20 g, 0.131 mol) dissolved in 50 mL of DMF was then added stepwise. After the addition was completed, the reaction mixture was stirred for 30 min, then cooling and the nitrogen atmosphere were stopped, and the reaction mixture was sealed and left overnight. Then, 500 mL chloroform was added and the mixture was washed with 4 × 200 mL of a saturated solution of $KHSO_4$ and 4 × 200 mL of TDW (the solid that precipitates during the washings is also collected with the organic layer). The organic layer was evaporated, and the product (that contained DMF traces) was precipitated by adding 300 mL of TDW and stirring for a few minutes. The product was collected by filtration and dried by suction and then in vaccue. The crude product was purified as follows: 150 mL of $CHCl_3$ was added to the white solid, and the mixture was stirred for a few minutes. Two hundred milliliters of petroleum ether 40−60 was then added, and the solid was collected by filtration yielding 37.61 g (0.11 mol 82%) of white powder; mp 177−183 °C. ^{1}H NMR ($CDCl_3$, 300 MHz, 298 K): δ 2.24 (t, 2H), 2.46 (t, 2H), 7.18−7.48 (m, 15H). MS (ES): m/z 347.

Acm−Thiopropanoic Acid (9). Tritylthiopropanoic acid (**8**) (11.5 g, 0.033 mol) was dissolved in 50 mL of TFA. The solution was stirred for 30 min, and an additional 15 mL of TFA was added during this period. Acetamidomethanol (3.088 g, 0.035 mol) dissolved in 15 mL of TFA was then added, and the reaction mixture was stirred for an additional 2.5 h. Most of the TFA was evaporated, and 150 mL of TDW was added; the precipitate formed was filtered. The filtrate was brought to pH 3−4 using Na_2CO_3 and was saturated with NaCl. The product was extracted to 6 × 80 mL of chloroform:2-propanol (3:1), and the organic phase was dried by Na_2SO_4 and evaporated to yield 1 g (0.0056 mol 17.1%) of white oil. ^{1}H NMR (CD_3OD, 300 MHz): δ 1.96 (s, 3H) 2.62 (t, 2H), 2.82 (t, 2H), 4.31 (s, 2H).

Peptide Synthesis. All peptides (except analogue 4) were synthesized on Rink amide methylbenzhydrylamine (MBHA) resin (0.64 mmol/g). Seven grams of resin was preswollen for 2 h in *N*-methylpyrrolidone (NMP) by shaking in a reaction vessel equipped with a sintered glass bottom. The Fmoc protecting group was removed from the resin by reaction with 20% piperidine in NMP (2 × 30 min each). Following Fmoc removal, the resin was washed with NMP (5 × 2 min) and dichloromethane (DCM) (2 × 2 min). Fmoc removal was monitored by the qualitative Ninhydrin test (Kaiser test).[25] A coupling cycle was carried out as follows: Fmoc-GlyS2(Acm)-OH (3 equiv), PyBroP (3 equiv), and diisopropylethylamine (DIEA) (6 equiv) in NMP were preactivated for 10 min, and the mixture was poured into the resin and mixed for 2 h at room temperature. Reaction completion was monitored by the Ninhydrin test. Following coupling, the building unit resin was washed with NMP (5 × 2 min) and DCM (2 × 2 min). Capping was carried out by reaction of the building unit resin with acetic anhydride (0.5 M), DIEA (0.125 M) and *N*-hydroxybenzotriazole (HOBt) (0.015 M) in DMF for 30 min at room temperature. After the resin was capped, NMP and DCM washes were carried out as above. Fmoc removal was carried out as described above. Fmoc-Phe-OH was coupled following activation as above (Xaa (3 equiv), PyBroP (3 equiv), DIEA (6 equiv), NMP 2 h). Fmoc removal and the washing step were carried out as above. The peptidyl resin was washed as above. Fmoc-Thr(*t*Bu)-OH was coupled to the peptidyl resin as described above. Coupling was monitored by the Ninhydrin test. The peptide was elongated by repeating washings/deprotection/washings/coupling as described above. After the coupling of the second Fmoc-Phe-OH, the resin was dried and split into 6 portions of 1 g each and the proceeding couplings took place separately.

1. Analogue 5. Following Fmoc removal, Fmoc-Cys(Acm)-OH was coupled twice {preactivation: (Fmoc-Cys(Acm)-OH (3 equiv), PyBroP (3 equiv), DIEA (6 equiv)} and monitored by the Ninhydrin test. Following Fmoc removal, Fmoc-DPhe-OH was coupled as described above, and the coupling was repeated using Fmoc-DPhe-OH (5 equiv), HOBt (5 equiv), and *N*,*N*-diisopropylcarbodiimide (DIC) (5 equiv) in DMF:DCM (1:1) for 1 h (monitored by Ninhydrin test). The resin was washed with NMP (3 × 2 min) and DMF:H_2O (4:1) (3 × 2 min). Cyclization was carried out with I_2 (5 equiv) in DMF:H_2O (4:1) at room temperature for 40 min. The peptidyl resin was washed with DMF (2 × 2 min), 2% ascorbic acid in DMF (2 × 2 min), NMP (5 × 2 min), and DCM (2 × 2 min). Following Fmoc removal, the peptidyl resin was washed with NMP (5 × 2 min) and DCM (2 × 2min) and cleaved from the resin by reaction with a precold mixture of TFA (95%), triisopropylsilane (TIS) (2.5%), and H_2O (2.5%) at 0 °C for 30 min and for 2.5 h at room temperature. The resin was removed by filtration and washed with TFA (2 × 5 mL); combined filtrates were evaporated under a stream of nitrogen. The oily product was triturated with cold ether, and the ether was decanted. The precipitate was washed with cold ether several times. A white powder was obtained. This crude product was dried. The weight of the crude product was 318 mg.

2. Analogue 6. Following Fmoc removal, Fmoc-GlyS2(Acm)-OH (3 equiv) was coupled at room temperature for 2 h {after preactivation with PyBroP (3 equiv) and DIEA (6 equiv) in NMP for 10 min}. Reaction completion was monitored by the Ninhydrin test. Cyclization was carried out with I_2 (10 equiv) in DMF:H_2O (4:1) at room temperature for 40 min as described above. The peptidyl resin was washed as above. Following Fmoc removal, the peptidyl resin was washed with NMP (5 ×

2 min) and DCM (2 × 2 min), cleaved from the resin, and treated as described above. The weight of the crude product was 391 mg.

3. Analogue 7. Following Fmoc removal, Fmoc-GlyS2(Acm)-OH was coupled as described in analogue 6. Reaction completion was monitored by the Ninhydrin test. Following Fmoc removal, Fmoc-DPhe-OH (3 equiv) was coupled after preactivation with PyBroP (3 equiv) and DIEA (6 equiv) for 10 min and coupling at room temperature for 2 h. Cyclization and the washing steps were carried out as described for analogue 6. Following Fmoc removal, the peptide resin was washed with NMP (5 × 2 min) and DCM (2 × 2 min), cleaved from the resin, and treated as described above. The weight of the crude product was 467 mg.

4. Analogue 8. Following Fmoc removal, Fmoc-GlyS2(Acm)-OH was coupled as described for analogue 6. Reaction completion was monitored by the Ninhydrin test. Following Fmoc removal, Fmoc-D-2-Nal (3 equiv) was coupled after preactivation with PyBroP (3 equiv) and DIEA (6 equiv) for 10 min and coupling at room temperature for 2 h. Cyclization and the washing steps were carried out as described for analogue 6. Following Fmoc removal, the peptidyl resin was washed with NMP (5 × 2 min) and DCM (2 × 2 min), cleaved from the resin, and treated as described above. The weight of the crude product was 447 mg.

5. Analogue 2. Following Fmoc removal, Acm−thioacetic acid was coupled using Acm−thioacetic acid (3 equiv), PyBroP (3 equiv), and DIEA (6 equiv) at room temperature for 2 h after preactivation for 10 min. The coupling was repeated with Acm−thioacetic acid (5 equiv), HOBt (5 equiv), and DIC (5 equiv) in DMF:DCM (1:1) for 1 h and monitored by the Ninhydrin test. Cyclization, washings, and cleavage were carried out as described above. The weight of the crude product was 264 mg.

6. Analogue 3. Following Fmoc removal, Acm−thiopropionic acid was coupled using Acm−thiopropionic acid (8.8 equiv), PyBroP (8.8 equiv), and DIEA (17.7 equiv) at room temperature for 2 h after preactivation for 10 min. Reaction completion was monitored by the Ninhydrin test. Cyclization, washings, and cleavage were carried out as described above. The weight of the crude product was 377 mg.

7. Analogue 4. Rink amide MBHA resin (1.5 g) (0.55 mmol/g) was preswollen for 2 h in NMP while shaking in a reaction vessel equipped with a sintered glass bottom. The Fmoc protecting group was removed from the resin by reaction with 20% piperidine in NMP (2 × 30 min). Fmoc removal was monitored by the Ninhydrin test. A coupling cycle was carried out with Fmoc-GlyS2(Acm)-OH (3 equiv), PyBroP (3 equiv), and DIEA (7 equiv) in NMP at room temperature for 2 h, after preactivation for 10 min. Following coupling, the peptidyl resin was washed with NMP (5 × 2 min) and DCM (2 × 2 min). Reaction completion was monitored by the Ninhydrin test. Capping was carried out by reaction of the peptidyl resin with acetic anhydride (0.5 M), DIEA (0.125 M), and HOBt (0.015 M) in DMF for 30 min at room temperature. After capping, NMP and DCM washes were carried out as above. Fmoc removal and washing steps were carried out as described above. Fmoc-Phe-OH was coupled as described above. Fmoc removal was monitored by the Ninhydrin test. All of the Xaa from this part until coupling of the Fmoc-Cys(Acm)-OH (including couplings, Fmoc removals, washing steps, and Ninhydrin tests) were carried out as described above. After the coupling of Fmoc-Cys(Acm)-OH, the resin was dried and split into two portions of 750 mg each and cyclization was carried out separately on each portion. Cyclization of the first portion was carried out with $Tl(CF_3CO_2^-)_3$ (1.2 equiv) in DMF at 5 °C for 80 min. The peptidyl resin was washed with DMF (5 × 2 min) and DCM (2 × 2 min). Following Fmoc removal, the peptide resin was washed with NMP (5 × 2 min) and DCM (2 × 2 min), cleaved from the resin, and treated as described above. Cyclization of the second portion was carried out with I_2 (10 equiv) in DMF:H_2O (4:1) at room temperature for 40 min. The peptidyl resin was washed with DMF (2 × 2 min), 2% ascorbic acid in DMF (2 × 2 min), NMP (5 × 2 min), and DCM (2 × 2 min). Following Fmoc removal, the peptide resin was washed with NMP (5 × 2 min) and DCM (2 × 2 min), cleaved from the resin, and treated as described above. After analytical HPLC, the crude products were combined and weighed 380 mg.

The crude peptides were purified by reversed-phase preparative HPLC. Fractions were analyzed by HPLC, and relevant fractions were combined. The product obtained from freeze-drying of the combined fractions showed a single peak in HPLC.

The presence of mass of the desired peptide was confirmed with mass spectrometric analysis performed on a VG-Platform II using electrospray ionization in positive and/or negative mode, as appropriate. The molecular masses of all of the peptides as determined by MS were in agreement with the calculated masses.

Radioligand Binding Assays. Radioligand binding assays were carried out on membranes prepared from CHO-K1 cells stably expressing individually cloned somatostatin receptors. Cells were grown for 2 days for almost confluence and were washed and scraped into 50 mM ice-cold Tris-HCl, pH 7.8, containing 1 mM EGTA, 5 mM $MgCl_2$, 10 mg/mL leupeptin, 200 mg/mL bacitracin, 0.1 mM PMSF, and 0.5 mg/mL aprotinin (buffer A) and were centrifuged at 10 000 rpm for 10 min at 4 °C (in Sorvall RC 26 Plus ultracentrifuge, rotor SS-34). The pellet was resuspended in buffer A and homogenized with a Polytron PT 1200 homogenizer (Kinematica AG, Switzerland) (setting 2, 3 strokes 10 s each). The homogenate was then centrifuged at 20 000 rpm for 20 min at 4 °C. The pellet was resuspended in buffer A and homogenized using the Polytron homogenizer (setting 2, 3 strokes 5 s each). The protein content was determined by Bradford, and the membrane preparation was diluted in buffer A containing 1 mg/mL bovine serum albumin (BSA) to a final 0.2 or 0.4 mg/mL membrane protein (depending on the specific somatostatin receptor used).

The radioligand binding assay was performed in 96 well microtiter plates (Maxisorp plates, Nunc, Denmark). Cell membranes (10 or 20 mg protein) were incubated with ^{125}I-Tyr^{11} somatostatin-14 (0.05 mCi; specific activity 2000 Ci/mmol), in a final volume of 250 mL, for 45 min at room temperature in the presence or absence of competing peptides. Nonspecific binding was defined as the radioactivity remaining bound in the presence of 1 mM somatostatin. At the end of the binding, reaction free radioligand was separated from bound ligand by rapid filtration through UniFilter GF/C plates preincubated in a solution of 5 g/L polyethyleneimine and 1 g/L BSA. The filtration was performed in FilterMate Cell Harvester (Packard Instrument Company, U.S.A.). After filtration, the filters were washed several times with cold buffer A containing 1 mg/mL BSA and allowed to dry overnight at room temperature. Then, 50 mL of scintillation liquid was added to each filter, and bound radioactivity was counted in a TopCount MicScintillation Counter (Packard). The binding assays were performed in triplicate wells. All experiments were performed at least twice. Displacement experiments, in which tested compounds displaced the binding of ^{125}I-Tyr^{11} somatostatin-14 with an IC_{50} value less than 100 nM, were repeated three times. Data from radioligand binding were used to generate inhibition curves, and IC_{50} values were determined for each of the tested peptides. The saturation binding data were analyzed by the method of Scatchard, and IC_{50} values are expressed as mean ± SEM (standard error of the mean).

Metabolic Stability. The metabolic stability of the backbone cyclic analogues was determined by incubation of the pure analogues with various tissue enzyme mixtures. Briefly, peptides were incubated at a final concentration of 0.4 mg/mL in rat liver homogenate or rat renal homogenate for up to 4 h at 37 °C. Samples were withdrawn at several time intervals, and the percentage of the unchanged molecules was analyzed by HPLC. Degradation of peptide was verified by the apparent reduction of the area under the curve of the chromatogram major peak. Degradation was confirmed by newly

emerging peaks (i.e., fragments) that were derived from the peptide as compared to the control blank chromatogram. All experiments were repeated three times; the data were expressed as mean ± SEM. The comparisons between groups were analyzed by one way analysis of variance for repeated measures at the 95% confidence level.

Acknowledgment. This study was financed by Peptor Ltd., Rehovot Israel. S.G. thanks Dr. Joseph Salitra, Dr. Tami Yechezkel, Dr. Asher Algawi, Dr. Eliezer Falb, Dr. Dvira Shohat, Dr. Erez Gur, Mrs. Manuela Lazarov, and Mrs. Elana Hariton for their helpful discussions. Special thanks to Dr. Nurit Livnah and Dr. Assaf Friedler for their critical review of this work.

Supporting Information Available: The MS and amino acid analysis of analogues 2−8 (Figure 1). This material is available free of charge via the Internet at http://pubs.acs.org.

References

(1) Kishore, R.; Raghothama, S.; Balaram, P. Cystine peptides: the intramolecular antiparallel beta-sheet conformation of a 20-membered cyclic peptide disulfide. *Biopolymers* **1987**, *26*, 6, 873−891.

(2) Toniolo, C. Structure of conformationally constrained peptides: from model compounds to bioactive peptides. *Biopolymers* **1989**, *28*, 247−257.

(3) Brazeau, P.; Vale, W. W.; Burgus, R.; Ling, N.; Butcher, M.; Rivier, J.; Guillemin, R. Hypothalamic polypeptide that inhibits the secration of immunoreactive pituitary growth hormone. *Science* **1973**, *179*, 77−79.

(4) Gilon, C.; Halle, D.; Chorev, M.; Selinger, Z.; Byk, G. Backbone cyclization: a new method for conferring conformational constraint on peptides. *Biopolymers* **1991**, *31*, 745−750.

(5) Saulitis, J.; Mierke, D. F.; Byk, G.; Gilon, C.; Kessler, H. Conformation of cyclic analogues of substance P: NMR and molecular dynamics in dimethyl sulfoxide. *J. Am. Chem. Soc.* **1992**, *114*, 4818−4827.

(6) Conradi, R. A.; Hilgers, A. R.; Ho, N. F. H.; Burton, P. S. The influence of peptide structure on transport across Caco-2 cells II. Peptide bond modification which results in improved permeability. *Pharm. Res.* **1992**, *9*, 435−439.

(7) Samanen, J.; Wilson, G.; Smith, P. L.; Lee, C.-P.; Bondinell, W.; Ku, T.; Rhodes, G.; Nichols, A. Chemical approaches to improve the oral bioavialability of peptidergic molecules. *J. Pharm. Pharmacol.* **1996**, *48*, 119−135.

(8) Grdadolnik, S. G.; Mierke, D. F.; Byk, G.; Zeltser, I.; Gilon, C.; Kessler, H. Comparison of the conformation of active and nonactive backbone cyclic analogues of substance P as a tool to elucidate features of the bioactive conformation. NMR and molecular dynamics in DMSO and water. *J. Med. Chem.* **1994**, *37*, 2145−2152.

(9) Bitan, G.; Behrens, S.; Matha, B.; Mashriki, Y.; Hanani, M.; Kessler, H.; Gilon, C. New backbone cyclic substance P analogues. *Lett. Pept. Sci.* **1995**, *2*, 121−124.

(10) Alstein, M.; Ben-Aziz, O.; Daniel, S.; Schefler, I.; Zeltser, I.; Gilon, C. Backbone cyclic peptide antagonists, derived from the insect pheromone biosynthesis activating neuropeptide, inhibit sex pheromone biosynthesis in moths. *J. Biol. Chem.* **1999**, *274*, 17573−17579.

(11) Bitan, G.; Zeltser, I.; Byk, G.; Halle, D.; Mashriki, Y.; Gluhov, E.; Sukhotinski, I.; Hanani, M.; Selinger, Z.; Gilon, C. Backbone Cyclization of the C-terminal Part of Substance P: the Important Role of the Sulfur in Position 11. *J. Pept. Sci.* **1996**, *2*, 261−269.

(12) Bitan, G.; Sukhotinsky, I.; Mashriki, Y.; Hanani, M.; Selinger, Z.; Gilon, C. Synthesis and Biological Activity of Novel Backbone-Bicyclic Substance-P Analogues Containing Lactam and Disulfide Bridges. *J. Pept. Res.* **1997**, *49*, 421−426.

(13) Reichlin, S.; Somatostatin: Historical aspects. *Scand. J. Gastroenterol.* **1986**, *21*, (Suppl. 119), 1−10.

(14) Reisine, T.; Bell, G. I. Molecular biology of somatostatin receptors. *End. Rev.* **1995**, *16*, 4, 427−442.

(15) Rossowski, W.; Gu, Z.-F.; Akarca, U.; Jensen, R.; Coy, D. Charectarization of somatostatin receptor subtypes controlling rat gastric acid and pancreatic amylase release. *Peptides* **1994**, *15*, 8, 1421−1424.

(16) Veber, D.; Freidinger, R.; Schwenk, D.; Palavede, W.; Holly, F.; Strachan, R.; Nutt, R.; Arison, B.; Hammnich, C.; Randall, W.; Glitzer, M. Saperstien, R.; Hirschmann, R. A potent cyclic hexapeptide analogue of somatostatin. *Nature* **1981**, *292*, 55−58.

(17) Lamberts, S. W.; Lely, A. J. V. D.; Herder, W. W. D.; Hofland, L. J. Octreotide. *N. Engl. J. Med.* **1996**, *334*, 4, 246−254.

(18) Afargan, M.; Janson, E. T.; Gelerman, G.; Rosenfeld, R.; Ziv, O.; Karpov, O.; Wolf, A.; Bracha, M.; Shohat, D.; Liapakis, G.; Gilon, C.; Hoffman, A.; Stephensky, D.; Oberg, K. Novel long-acting somatostatin analogue with endocrine selectivity: potent suppression of growth hormone but not of insulin. *Endocrinology* **2001**, *142*, 1, 477−486.

(19) Albericio, F.; Royo, M.; Munson, M. C.; Solé, N. A.; Abel, R. J. V.; Alsina, J.; García-Echeverria, C.; Slomczyńska, U.; Eritja, R.; Pons, M.; Giralt, E.; Barany, G. Strategies and tactics for the solid-phase synthesis of cystine-containing peptides. *Peptide Chemistry*; Escom: Leiden, The Netherlands, 1992; pp 19−23.

(20) Kamber, B.; Hartman, A.; Eisler, K.; Riniker, B.; Rink, H.; Sieber, P.; Rittel, W. The synthesis of cystin peptides by iodine oxidation of S-trityl-cystein and S-acetamidomethyl-cystein peptides. *Helv. Chim. Acta* **1980**, *63*, 899−915.

(21) Rossowsky, W. J.; Coy, D. H. Specific inhibition of rat pancreatic insulin or glucagon release by receptor-selective somatostatin analogues. *Biochem. Biophys. Res. Commun.* **1994**, *205*, 1, 341−346.

(22) Rohrer, S. P.; Birzin, E. T.; Mosley, R. T.; Berk, S. C.; Hutchins, S. M.; Shen, D.-M.; Xiong, Y.; Hayes, E. C.; Parmar, R. M.; Foor, F.; Mitra, S. W.; Degrado, S. J.; Shu, M.; Klopp, J. M.; Cai, S.-J.; Blake, A.; Chan, W. W. S.; Pasternak, A.; Yang, L.; Patchett, A. A.; Smith, R. G.; Chapman, K. T.; Schaeffer, J. M. Rapid identification of subtype selective agonists of somatostatin receptor through combinatorial chemistry. *Science* **1998**, *282*, 737−740.

(23) Pasternak, A.; Pan, Y.; Mario, D.; Sanderson, P. E.; Mosley, R.; Roher, S. P.; Birzin, E. T.; Huskey, S. E. W.; Jacks, T.; Schleim, K. D.; Schaeffer, J. M.; Patchett, A. A.; Yang, L. Potent, orally bioavailable somatostatin agonists: good absorption achieved by urea backbone cyclization. *Bioorg. Med. Chem. Lett.* **1999**, *9*, 491−496.

(24) Fujii, N.; Otaka, A.; Funakoshi, S.; Bessho, K.; Watanabe, T.; Akaji, K.; Yajima, H. Studies on peptides. CLI. Syntheses of cystine-peptides by oxidation of S-protected cystein-peptides with thallium (III) trifluoroacetate. *Chem. Pharm. Bull.* **1987**, *35*, 2339−2347.

(25) Kaiser, E.; Colescold, D. C.; Bossinger, C. D.; Cook, P. Color test for detection of free terminal amino groups in the solid-phase synthesis of peptides. *Anal. Biochem.* **1970**, *34*, 595.

JM0100281